Effect of sea-level on organic carbon preservation in the Okinawa Trough over the last 91 kyr

Article *in* Marine Geology · March 2018
DOI: 10.1016/j.margeo.2018.02.013

6 authors, including:

Dawei Li
Ocean University of China
19 PUBLICATIONS **44** CITATIONS
SEE PROFILE

Qian Li
Xiamen University
15 PUBLICATIONS **170** CITATIONS
SEE PROFILE

Li-Wei Zheng
Xiamen University
18 PUBLICATIONS **31** CITATIONS
SEE PROFILE

Xiaodong Ding
Xiamen University
6 PUBLICATIONS **10** CITATIONS
SEE PROFILE

Marine Geology 399 (2018) 148–157

Contents lists available at ScienceDirect

Marine Geology

journal homepage: www.elsevier.com/locate/margo

Effect of sea-level on organic carbon preservation in the Okinawa Trough over the last 91 kyr

Da-Wei Li[a,1], Yuan-Pin Chang[b], Qian Li[a], Liwei Zheng[a], Xiaodong Ding[a], Shuh-Ji Kao[a,*]

[a] State Key Laboratory of Marine Environmental Science, Xiamen University, Xiamen 361102, China
[b] Department of Oceanography, National Sun Yat-sen University, 70 Lien-hai Road, Kaohsiung 806, Taiwan

ARTICLE INFO

Keywords:
Core MD012404
Reactive phosphorus
Productivity
Redox change
Organic carbon burial efficiency

ABSTRACT

The burial of marine organic carbon, primarily synthesized by marine autotrophic organisms, into sediment removes CO_2 from the ocean-atmosphere system. However, linkages between export productivity and organic carbon burial and the controlling factors remained ambiguous, especially for marginal seas. In this study, we measured redox-sensitive trace metal concentrations and planktic foraminifer fauna assemblages for a sediment core collected from the middle Okinawa Trough spanning the past 91 kyr. Through compilation with other published data, we found that the export productivity was decoupled from organic carbon burial. Variability of manganese and total sulfur contents suggested that both bottom water and surface sediment had experienced significant redox change in the last glacial cycle. By using the ratio of marine organic carbon to reactive phosphorus, i.e., $OC_{marine}/P_{react.}$, we reconstructed organic carbon burial efficiency which showed relatively higher values during the last glacial and low values during the middle-late Holocene. After synthesizing our new and reported data, we conclude that the middle Okinawa Trough bottom water redox state was controlled by deep water ventilation induced by sea level change and related Kuroshio Current intrusion, instead of by the oxygen consumption owing to local export productivity.

1. Introduction

The marine soft-tissue pump (STP), through which dissolved inorganic carbon (DIC) is transformed into organic matter by photosynthesis and a portion of this organic carbon sinks into the deep ocean, plays an important role in regulating atmospheric CO_2 partial pressure (Cartapanis et al., 2016; Martínez-García et al., 2014; Sigman and Boyle, 2000). For the global ocean, although sedimentary organic carbon burial flux, which is ultimately removed from active carbon reservoirs (e.g., atmosphere and ocean), only accounts for about 0.5% of euphotic zone primary production (Hedges and Keil, 1995), the long-term storage of organic carbon in marine sediments plays a critical role in earth's carbon cycle, e.g., regulating atmospheric CO_2, on glacial and millennial time scales (Arndt et al., 2013; Burdige, 2007; Cartapanis et al., 2016; Roth et al., 2014). Recently, global marine organic carbon burial over the past 150 kyr have been reported by Cartapanis et al. (2016, and references therein), in which a general scenario that glacial organic carbon burial was ca. 50% higher than that of interglacial was proposed. However, temporal evolutions of organic carbon burial and export productivity display distinctly regional differences. For example, the phenomenon that glacial high export productivity coupled with higher organic carbon burial was observed in the subantarctic zone of the Southern Ocean and the Atlantic Ocean (Cartapanis et al., 2016; Kohfeld et al., 2005; Martínez-García et al., 2014); whereas enhanced glacial organic carbon burial was decoupled with productivity in much of the North Pacific marginal regions (Cartapanis et al., 2016; Kohfeld and Chase, 2011; Li et al., 2017b; Winckler et al., 2016). In addition, a recent research carried out in the equatorial Pacific divergent region also revealed that higher export productivity had occurred in the Holocene rather than in the last glacial stage (Costa et al., 2017), but organic carbon burial flux displays the contrary pattern (Cartapanis et al., 2016). Thus, the variability of organic carbon burial on glacial-interglacial time scale might be environment-specific, especially in marginal seas occupied by large variability of primary productivity and distinctive environmental factors, e.g., sedimentation rate and deep water ventilation. To better understand the mechanisms for global organic carbon burial and predict the future trend, information from different geographic areas and time scales is required.

In the modern ocean, marginal seas bury about 138 Tg (1 Tg = 10^{12} g) organic carbon per year, accounting for up to 90% of

* Corresponding author.
E-mail address: sjkao@xmu.edu.cn (S.-J. Kao).
[1] Present address: Key Laboratory of Marine Chemistry Theory and Technology (Ocean University of China), Ministry of Education, Qingdao 266100, China.

https://doi.org/10.1016/j.margeo.2018.02.013
Received 14 July 2017; Received in revised form 10 January 2018; Accepted 26 February 2018
Available online 07 March 2018
0025-3227/

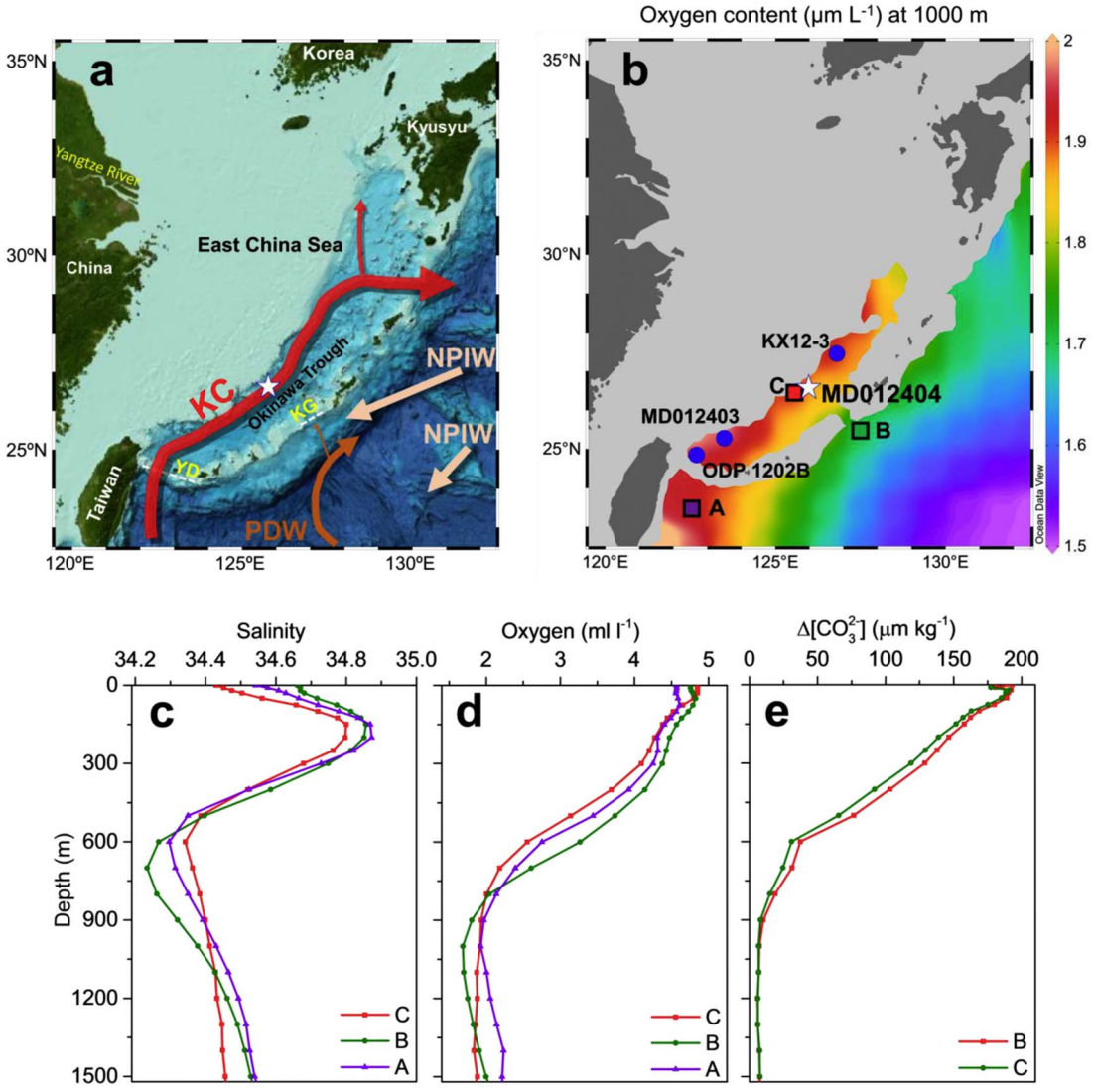

Fig. 1. Modern oceanographic context in and around the Okinawa trough. a, Topography with major water currents referred in this study. KC: Kuroshio Current; NPIW: North Pacific Intermediate Water; PDW: Pacific Deep Water. YD: Yonaguni Depression; KG: Kerama Gap. Map was created using data from GEBCO 2014 Grid (http://www.gebco.net/data_and_products/gridded_bathymetry_data/). b, Spatial distribution of dissolved oxygen concentrations at 1000 m isopleth. Oxygen data was taken from WOA2009 (http://www.nodc.noaa.gov/OC5/WOA09/woa09data.html). Site MD012404 for this study is labeled as white star, and other sites referred in this study are labeled as blue solid circles. Maps were generated by Ocean Data View software (Schlitzer, 2016). Vertical profiles are salinity (c), dissolved Oxygen (d) and $\Delta[CO_3^{2-}]$ (e) of selected sites (labeled as squares in b). $\Delta[CO_3^{2-}]$ was calculated following the method described in Yu and Elderfield (2007). Salinity and temperature data source from WOA2009 (http://www.nodc.noaa.gov/OC5/WOA09/woa09data.html). (For interpretation of the references to color in this figure legend, the reader is referred to the web version of this article.)

marine sedimentary organic carbon burial (Hedges and Keil, 1995); meanwhile, more than 50% of marginal seas/basins are concentrated in the western Pacific (Tamaki and Honza, 1991; Wang, 1999). Coupled abundant riverine inputs with high sedimentation rate, western Pacific marginal seas/basins may serve as an important deposit for organic carbon, potentially playing an important role in the global carbon cycle. The Okinawa Trough lies between the East China Sea Shelf and the Ryukyu arc (Fig. 1a), with maximum water depth greater than 2000 m in the southern part. With numerous rivers in the surrounding area, e.g., the Yangtze River, Yellow River, and mountainous rivers in Taiwan Island (not shown in Fig. 1), the Okinawa Trough received large amounts of detrital sediments during the late Quaternary, providing high resolution sedimentary records for deciphering paleo-climate and paleo-environment changes on orbital and millennial time scales (Chang et al., 2008, 2009; Chen et al., 2010; Dou et al., 2015; Jian et al., 2000; Kao et al., 2005, 2006a; Shao et al., 2016; Ujiié et al., 2016; Xiang et al., 2007; Zheng et al., 2016). During the last two decades, several studies were carried out for reconstructions of export productivity and organic carbon burial in the Okinawa Trough (Chang et al., 2009; Dou et al., 2015; Jian et al., 1996; Li et al., 2005; Li et al., 2017b; Ruan et al., 2017; Shao et al., 2016; Xu et al., 2012). However, conflicts have been noted between estimates of export productivity and organic carbon burial. For instance, relatively higher total organic carbon (TOC) content was observed in the southern Okinawa Trough during the last glacial and deglacial stages (Amano and Itaki, 2016; Kao et al., 2005, 2006a; Ujiié et al., 2001), whereas contemporary biogenic-barium (bio-Ba, export productivity proxy) was in lower state (Dou et al., 2015; Kao et al., 2005; Shao et al., 2016). This disagreement might be caused by the variability of environmental redox changes considering that organic matter is sensitive to diagenesis within the sediment. Although plenty of studies have reported paleo-environmental changes in the Okinawa Trough covering the interval from the last glacial maximum to the Holocene (Amano and Itaki, 2016; Dou et al., 2015; Kao et al., 2006a, 2006b; Li et al., 2005), the variations of redox condition and organic carbon burial efficiency in the Okinawa Trough remain unclear.

In this study, biogenic and redox sensitive metal elements were analyzed and foraminifer fauna abundance data were generated from site MD012404 located in the middle Okinawa Trough. Combined with published data including phosphorus, TOC and its stable carbon isotope, biogenic opal, foraminifera, $CaCO_3$ and total sulfur from the same site, we re-evaluate production proxies, and discuss potential environmental factors influencing the carbon burial in the middle Okinawa Trough over the last glacial-interglacial cycle.

2. Modern hydrographic setting in the Okinawa Trough

As part of the North Pacific western boundary current, the Kuroshio Current enters the Okinawa Trough mainly via the Yonaguni Depression (sill depth ca. 775 m) to the east off Taiwan Island (Fig. 1a). Beside the Kuroshio Current, the North Pacific Deep Water (PDW), characterized by a dissolved oxygen minimum at about 1000 m water depth (Fig. 1b, d), serves as a source for Okinawa Trough bottom water (deeper than 800 m) entering through the Kerama Gap (sill depth of about 1100 m) (Nakamura et al., 2013). Between the two layers mentioned above, the Philippine Sea Intermediate Water, a mixture of North Pacific Intermediate Water (NPIW) and South China Sea Intermediate Water, intrudes into the Okinawa Trough from both the Yonaguni Depression and the Kerama Gap (Nakamura et al., 2013), resulting in a salinility minimum at about 600–700 m depth in the Okinawa Trough (Fig. 1c). Due to the diapycnal mixing induced by Kuroshio Current intrusion, which has a flow rate up to 100 cm s^{-1} (Liang et al., 2003), deep water between 800 and 1200 m contains relatively higher dissolved oxygen concentration in the middle Okinawa Trough than that in open ocean waters to the east of Kerama Gap (Fig. 1b, d).

3. Material and methods

3.1. Samples and age model

Core MD012404 (water depth 1397 m; 26°38.84′N, 125°48.75′E), with a total length of 43.67 m, was retrieved from the middle Okinawa Trough (Fig. 1b) during the IMAGES (International Marine Past Global Change) cruise in 2001 (Bassinot et al., 2002). Sediments in this core are mainly composed of nearly homogenous nannofossil ooze or diatom-bearing nannofossil as described by Chang et al. (2008) in detail. The age model for the upper 21.745 m was based on 17 Accelerator Mass Spectrometry ^{14}C ages of planktonic foraminifera (*G. sacculifer* and *G. ruber*) as described by Chang et al. (2009) in detail. For the older part (21.745–43.670 m), age model was established by graphically aligning the benthic foraminiferal $\delta^{18}O$ record from site MD012404 to the Pacific deep benthic foraminiferal $\delta^{18}O$ stack curve as described by Li et al. (2017b). In this study, metal elements were analyzed over the last 30 kyr. For metal analysis (total 62 samples), samples were taken at 20 to 40 cm intervals with an average resolution of 454 years per sample.

3.2. Chemical analysis

Sediments were rinsed twice with deionized distilled water to remove porewater salt and were then freeze-dried. For each sample, about 0.1 g freeze-dried sample along with an acid mixture of 0.5 ml $HClO_4$, 5 ml HF, and 5 ml HNO_3 (Suprapur grade from Merck) were placed into digestion vessel and microwaved. Afterwards, the remaining acid mixture was evaporated to dryness, and the dried sample was further redissolved in 2 ml HNO_3 and the solution was diluted, with Milli-Q water, to 20 ml (in 2% HNO_3). The digested solution was analyzed for manganese (Mn), magnesium (Mg) and aluminum (Al) using an ICP-OES (Optima 3200DV, Perkin-ElmerTM Instruments, USA) at Research Center for Environmental Changes, Academia Sinica (Taipei). Within ranges of our element detection, accuracy and precision for metal elements were within 5%. All containers used in the study were microwaved with 5 ml concentrated HNO_3 and 2 ml Milli-Q water for 30 min and subsequently rinsed thoroughly with Milli-Q water prior to use. More details were described in Hsu et al. (2003).

3.3. Calculation of marine sourced organic carbon

The $\delta^{13}C$ values of TOC from site MD012404 fluctuated in a narrower range from −21.8‰ to −20.6‰ (Kao et al., 2006a), thus the TOC was mainly marine-sourced. By using −20‰ (Hedges et al., 1997) and −25.6‰ (Wu et al., 2007) as marine and terrestrial $\delta^{13}C$-TOC end-members, respectively, we calculated marine sourced organic carbon (OC_{Marine}) content as follows:

$$[OC_{Marine}] \times \delta^{13}C_M + [OC_{terrestrial}] \times \delta^{13}C_T = [TOC] \times \delta^{13}C_{TOC}, \quad (1)$$

$$[TOC] = [OC_{Marine}] + [OC_{terrestrial}], \quad (2)$$

where $\delta^{13}C_M$ and $\delta^{13}C_T$ are carbon isotope end-members for marine and terrestrial organic carbon, respectively; $\delta^{13}C_{TOC}$ is the carbon isotope of TOC from site MD012404; $[OC_{terrestrial}]$ is the terrestrial organic carbon content; $[OC_{Marine}]$ is the marine sourced organic carbon content.

3.4. Pulleniatina obliquiloculata shell abundance

Planktic foraminifer fauna assemblages (FFA) from the last 38 kyr were reported by Chang et al. (2008). In this study, we added new data for the interval from 38 ka to 91 ka. Samples were taken at 10 cm to 40 cm intervals between 38 and 91 ka (112 samples in total). Samples were freeze-dried, and then washed through a 104 μm sieve to remove clay and nannofossil ooze. After drying at 50 °C overnight, samples were sieved through a 149 μm size fraction which contained more than 300 whole specimens for identifying and counting under a microscope. A total of 27 species of planktonic foraminifers was identified and only the abundance of *Pulleniatina obliquiloculata* (*P. obliquiloculata*) was used in this study. The abundance of *P. obliquiloculata*, abbreviated as POA, is defined as:

$$POA = 100 \times [P.\ obliquiloculata]/[\text{total planktonic foraminifers}], \quad (3)$$

where [*P. obliquiloculata*] is the number of whole *P. obliquiloculata* shells, and [total planktonic foraminifers] is the number of total planktonic foraminifers including 27 species identified in this study.

3.5. Foraminifer fragmentation index

The foraminifer fragmentation index (FFI) is a measure of the preservation of foraminifer shell and biogenic carbonate (Broecker and Clark, 1999). FFI data for the 0–38 ka interval had been reported by Chang et al. (2008). In this study, we added new data for the 38–91 ka interval and samples were taken at 10 cm to 40 cm intervals (112 samples in total). Foraminifer fragmentation index was calculated as:

$$FFI = 100 \times [WPF]/[WPF+Fragments], \quad (4)$$

where [WPF] is the number of whole planktonic foraminifers, and [WPF + Fragments] is total number of whole planktonic foraminifers and fragments larger than 104 μm.

3.6. Carbonate saturation state, $\Delta[CO_3^{2-}]$

Given that we applied the biogenic $CaCO_3$ record to infer productivity change, the potential biogenic $CaCO_3$ dissolution (carbonate saturation state) in the modern-day water column was assessed for areas adjacent Okinawa Trough (Fig. 1e). Using parameters including pressure (water depth), micro-nutrients, water temperature, salinity, total CO_2 (μmol kg^{-1}), and alkalinity (μmol kg^{-1}), the vertical profile of $\Delta[CO_3^{2-}]$ ($\Delta[CO_3^{2-}] = [CO_3^{2-}]_{in\text{-}situ} - [CO_3^{2-}]_{saturation}$, Fig. 1e) was calculated following the methods described in Yu and Elderfield

(2007). Seawater CO_2 system was estimated using CO_2sys.xls (ver. 12) (Pelletier et al., 2005). Total alkalinity and total CO_2 were obtained from Global Ocean Data Analysis Project (GLODAP) (Key et al., 2004). Temperature, salinity, and nutrients (phosphate, nitrate and silicate) data used in the calculation were obtained from World Ocean Atlas (2009). The equilibrium constants, K_1 and K_2, for carbonic acid were obtained from Dickson and Millero (1987). Dissolution constants, K_B for boric acid, and K_{SO4} for the bisulfate ion, were obtained from Dickson (1990).

3.7. Other published records from core MD012404

Published biogenic records from core MD012404 were also synthesized in this study. Sedimentary opal content (Fig. 3d), mainly derived from diatoms and radiolarians, had been reported by Chang et al. (2009). Sedimentary TOC and carbonate contents had been reported by Chang et al. (2005). The planktonic foraminifera records including FFA, POA and FFI over the last 38 kyr had been reported by Chang et al. (2008). The total reactive phosphorous ($P_{react.}$, Fig. 3c), biogenic phosphorous components coupling with euphotic zone productivity, had been reported by Li et al. (2017b).

4. Results

4.1. Variations of metals over time

The contents of Al and Mg fall within the range of 6.90%–9.35%, and 1.36%–1.92%, respectively (Fig. 2a and b), with distinctly higher values during the last glacial-deglacial period and lower values in the Holocene. Contents of Fe (Fig. 2c) and Ti (Fig. 2d) have been reported by Li et al. (2017b), displaying similar pattern to that of Al and Mg over the last 30 kyr. The similar patterns of these four metal records result in relatively stable Mg/Al, Fe/Al and Ti/Al ratios over the last 28 kyr. The Mn contents (Fig. 2e) ranged from 0.05% to 0.10% and show a trend different to that of Al Mg, Fe and Ti. The Mn record experienced two low value intervals during 24–30 kyr and 14–18 kyr and high values during the last glacial maximum (LGM) and the Holocene. Variation of Mn/Al ratio (Fig. 2e, black) displays similar pattern to that of Mn content.

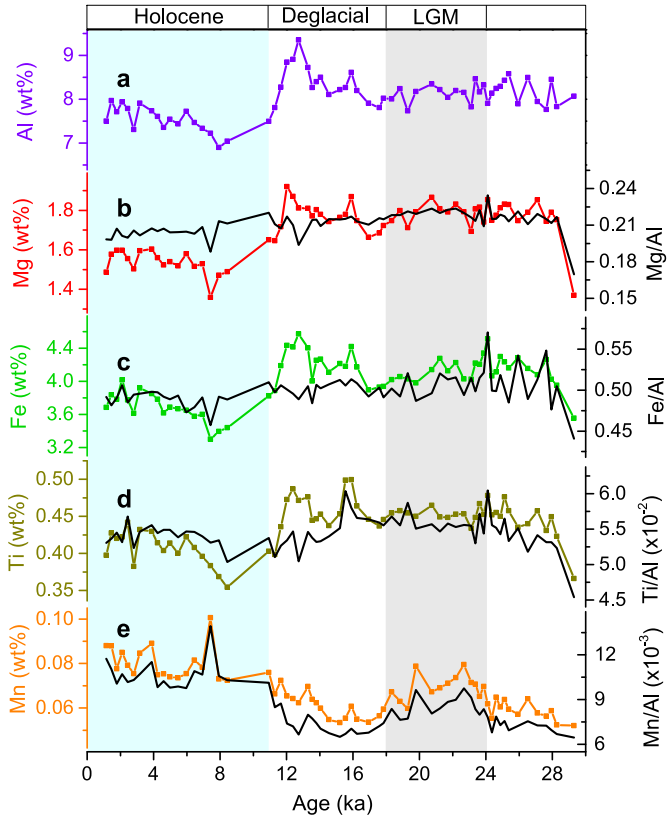

Fig. 2. Metal contents and Al normalized ratios from site MD012404. a, Al content (this study). b, Mg content (red) and Mg/Al ratio (black) (this study). c, Fe content (light green) and Fe/Al ratio (black) (Li et al., 2017b). d, Ti content (dark yellow) and Ti/Al ratio (black) (Li et al., 2017b). e, Mn content (orange) and Mn/Al (black) (this study). LGM: last glacial maximum. (For interpretation of the references to color in this figure legend, the reader is referred to the web version of this article.)

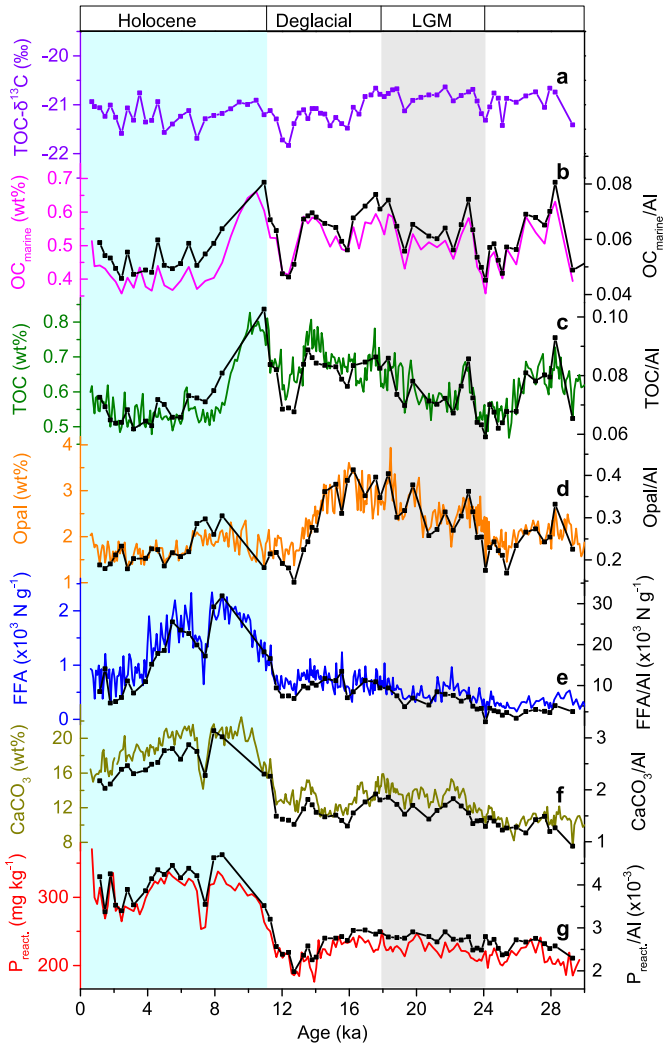

Fig. 3. Paleo-records from site MD012404 over the last 30 kyr. a, Carbon isotope of total organic carbon, TOC-δ^{13}C (Kao et al., 2006a). b, Calculated marine sourced organic carbon content, OC_{marine} (magenta, this study), and OC_{marine}/Al ratio (black, this study). c, TOC content (green, Chang et al., 2005) and TOC/Al ratio (black). d, Opal content (orange, Chang et al., 2008) and opal/Al ratio (black, this study). e, Total count of foraminiferal fauna assemblages, FFA (blue, Chang et al., 2008) and it's Al normalized ratio (black, this study). f, $CaCO_3$ content (dark yellow, Chang et al., 2005) and $CaCO_3$/Al ratio (black, this study). g, $P_{react.}$ content (red, this study) and $P_{react.}$/Al ratio (black, this study). LGM: last glacial maximum. (For interpretation of the references to color in this figure legend, the reader is referred to the web version of this article.)

4.2. Marine-sourced organic carbon

Over the last 30 kyr, calculated OC_{Marine} content (Fig. 3b, magenta line) falls in the range from 0.31% to 0.66%, accounting for ca. 81% (ranged from 67% to 89%) of sedimentary TOC. The OC_{Marine} record displayed higher values during intervals of 26–30 ka and 9–23 ka, and lowers values over the last 9 kyr. The content of OC_{Marine} displays

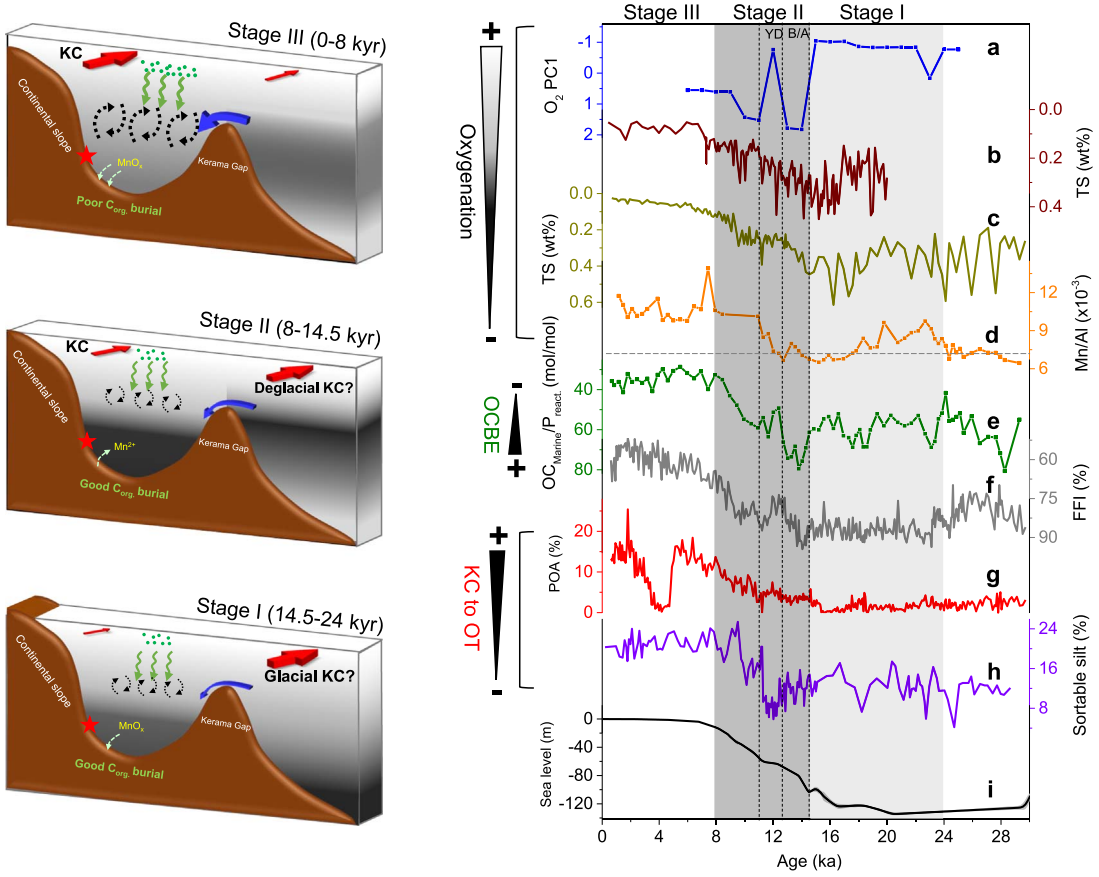

Fig. 4. Cartoons describing water oxygenation and ventilation in the OT (left), and paleo-records over the last 30 kyr (right). Left panel: Oxygenation state to the east off Kerama Gap was draw according to the results described by Galbraith and Jaccard (2015). Core MD012404 was labeled as red star. Dashed area with color from dark grey to white represents dissolved O_2 content from low (−) to high (+). KC: Kuroshio Current. OT: Okinawa trough. OCBE: organic carbon burial efficiency. Right panel: a, North Pacific benthic O_2 Principal Component 1, PC1, derived from sites shallower than 1500 m (Galbraith and Jaccard, 2015); positive value represents decreasing dissolved O_2 content and negative value suggests increasing dissolved O_2 content. b, Total sulfur (TS) content of site KX12-3 (Lim et al., 2017). c, TS content of site MD012404 (Kao et al., 2006a). d, Mn/Al ratio from site MD012404 (this study). Grey dashed line represents average upper continental crust Mn/Al ratio (McLennan, 2001). e, Marine soured organic carbon burial efficiency, OCBE, from site MD012404 (this study). f, Foraminifer fragmentation index, FFI (Chang et al., 2008). g, Abundance of planktonic *Pulleniatina obliquiloculata*, POA, from site MD012404 (Chang et al., 2008). h, Sortable silt fraction of core ODP1202 (Diekmann et al., 2008), used as a proxy for the Kuroshio Current intensity over the southern Okinawa Trough. i, Global sea level change (Lambeck et al., 2014). "+" and "–" in the left panel represent increase and decrease respectively. B/A: Bølling-Allerød; YD: Younger Dryas. (For interpretation of the references to color in this figure legend, the reader is referred to the web version of this article.)

similar temporal variations with TOC (Fig. 3c), yet, deviated from that of production records (Fig. 3), e.g., $CaCO_3$, reactive phosphorus and planktonic FFA.

4.3. Planktonic foraminiferal records

In this study, the carbonate saturation state was evaluated by $\Delta[CO_3^{2-}]$ in and surrounding Okinawa Trough. From Fig. 1e, it is observed that $\Delta[CO_3^{2-}]$ values of sites C (lies in Okinawa Trough) and B (to the east of Kerama Gap) are nearly the same at ~6.8 μmol kg^{-1} for water depth between 1000 m and 1500 m, suggesting that site MD012404 lies above the modern carbonate compensation depth (CCD).

P. obliquiloculata is the diagnostic indicator species of the Kuroshio Current in the western Pacific, and its abundance, i.e., POA, had been used to reconstruct the evolution of Kuroshio Current pathway shift as well as its intensity during the late Quaternary (Jian et al., 2000; Lin et al., 2006). During the past 91 kyr, POA falls in the range from 0 to 25.4%, with low values occurred during 14–24 ka and 60–70 ka (Figs. 4g, 5d). As for the foraminifer preservation index, FFI fell within the range of 51%–95% with higher values appeared during 14–24 kyr and 60–70 kyr, and lowest values in the late Holocene (Figs. 4f, 5e).

5. Discussions

To extract and reconstruct the productivity signal from sediment archives superimposed by *syn*- and post-depositional modifications is not an easy task in marginal seas, though it is critical to decipher the past carbon cycle. Sedimentary biogenic proxies including reactive phosphorus, TOC, $CaCO_3$, planktonic FFA, and opal are primarily controlled by ocean productivity and environmental processes that include remineralization (for organic proxies), and preservation/dissolution (for fauna assemblages and opal). By using reactive phosphorus, $CaCO_3$ and planktonic FFA as productivity proxies, and the redox sensitive metal as redox index, we intended to explore the effects of non-productivity factors and external forcing, such as mineral dilution and water column redox induced by water exchange or ventilation, on organic carbon burial in the middle Okinawa Trough.

5.1. Evaluation of marine productivity proxies (0–30 kyr)

The Okinawa Trough is characterized by active seafloor hydrothermal vents (Glasby and Notsu, 2003; Tsuji et al., 2012). Comparing with non-hydrothermal sediments, the Okinawa Trough hydrothermal sediments are significantly enriched (4–10 times higher) in Mg and Mn but depleted (3–50 times lower) in Fe and Ti (Shao et al., 2015; Zhai et al., 2007). During the past 30 kyr, Most of Mg/Al ratios (Fig. 2b) from

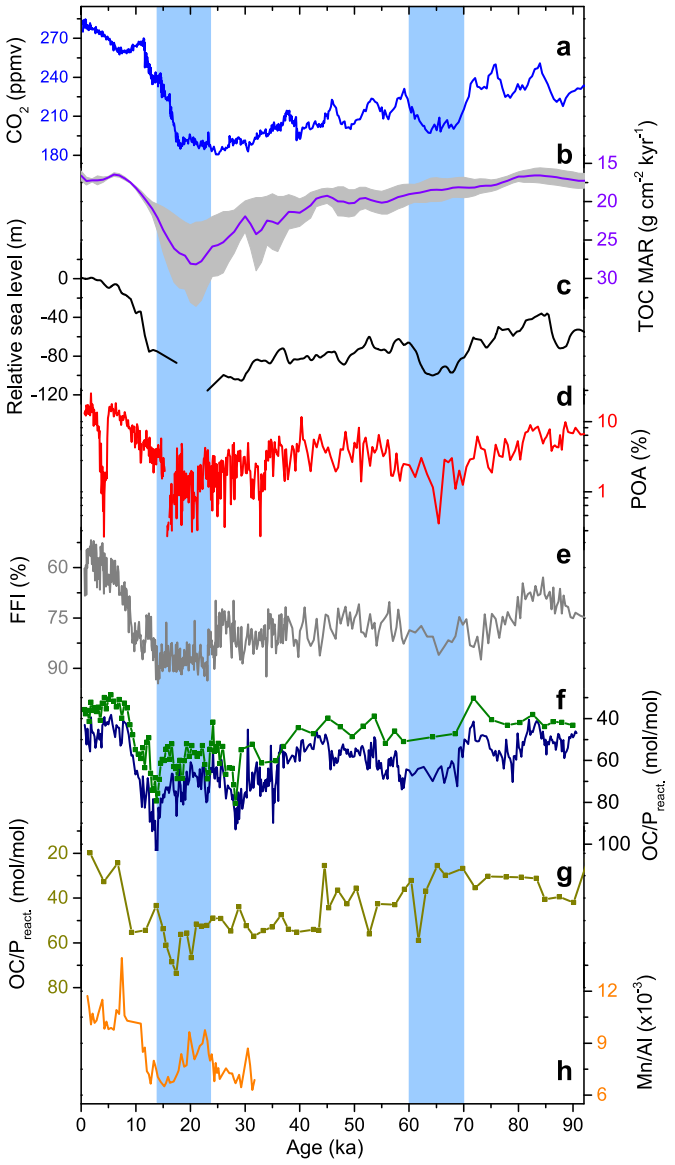

Fig. 5. Organic carbon preservation and related paleo-records over the last 91 kyr. a, Composite atmospheric CO_2 record from Antarctic ice cores (Bereiter et al., 2015). b, Global total organic carbon mass accumulation rate, TOC mass accumulation rate MAR (Cartapanis et al., 2016). c, Global sea level record (Grant et al., 2012). d, Abundance of planktonic *Pulleniatina obliquiloculata*, POA, from core MD012404. POA of 0–38 ka from Chang et al. (2008) and of 38–91 ka from this study. e, Foraminifer fragmentation index (FFI) from core MD012404. FFI of 0–38 ka from Chang et al. (2008) and of 38–91 ka from this study. f, Ratios of marine sourced organic carbon to reactive phosphorus, $OC_{marine}/P_{react.}$ (green line, this study), and total organic carbon to reactive phosphorus, $TOC/P_{react.}$ (navy line, this study). g, $TOC/P_{react.}$ ratio from ODP site 1144 (Tamburini et al., 2003). h, Mn/Al ratio from site MD012404 (this study). (For interpretation of the references to color in this figure legend, the reader is referred to the web version of this article.)

core MD012404 fell in the range of 0.198–0.225, similar to that of the Yangtze and Yellow river sediments, i.e., 0.207–0.231 (Yang et al., 2004), suggesting our sediment core experienced stable sediment source without significant influence of hydrothermal activity; In addition, the Fe/Al and Ti/Al ratios (Fig. 2c and d) from core MD012404 are stable and display similar values to that of the Yangtze and Yellow river sediments (Yang et al., 2004), lending further support to the postulation above. As proposed by Zheng et al. (2016), terrigenous sediments received by the middle Okinawa Trough mainly sourced from the Yangtze and Yellow rivers during the last glacial maximum through the Holocene. And the Al contents are similar in the upper continental crust of the Yangtze and Yellow river drainage basins (Gao et al., 1998).

By assuming that sedimentary Al was exclusively of terrestrial detrital origin and not affected by marine biological processes (Brumsack, 2006), detrital dilution effect can be eliminated by normalizing the M_{bio} to Al (M_{bio} represents biogenic proxies, e.g., TOC, reactive phosphorus or $CaCO_3$). For core MD012404, consistency in temporal variations between biogenic contents and their Al normalized ratios (Fig. 3) throughout the past 30 kyr suggests that dilution effect by terrestrial supply did not exert significant interference. We will use content data in the following discussion owing to their higher resolutions for more detail information. In general, three types of variations were identified from these biogenic records (Fig. 3). Opal record displayed higher values during the last glacial and deglaical stages with lower values during the Holocene. Oppositely, $P_{react.}$, $CaCO_3$ and FFA records showed higher values in the Holocene and lower values during the last glacial and deglaical stages. Content of TOC and OC_{Marine} values experienced relatively high value during the last glacial-deglacial and early Holocene but low value in the middle-late Holocene. Each biogenic record was evaluated in this section as follows.

Biogenic opal has been used to reconstruct total productivity in the Okinawa Trough by several studies (Chang et al., 2009; Dou et al., 2015; Shao et al., 2016). However, in subtropical regions including the Okinawa Trough, diatoms are - and likely were - only a minor component of the phytoplankton assemblage and hence their contribution to primary productivity may not reflect total productivity (Nelson et al., 1995). Thus, it is not convincing to use opal as a total (i.e., integrated) export productivity proxy in the oligotrophic subtropical regions such as the Okinawa Trough (see Supplementary materials).

Planktonic foraminifera are heterotrophic organisms that live on fresh organic matter (e.g., phytoplankton, small zooplankton, organic detritus etc.) originated from the euphotic zone photosynthesis (Spindler et al., 1984). Thus biomass/fauna assemblages of planktonic foraminifera should be positively correlated with export production. Core MD012404 lies above the modern CCD as indicated by positive $\Delta[CO_3^{2-}]$ values in middle Okinawa trough (Fig. 1e); In addition, better foraminifera preservation (lower percent of fragmentation, Fig. 4f) was observed in core MD012404 during glacial stage (Chang et al., 2008), ruling out the possibility that the glacial low carbonate contents were driven by enhanced dissolution during sinking downward process through the water column (Broecker and Clark, 1999). The total account of sedimentary planktonic FFA (Fig. 3e), including 27 identified species (Chang et al., 2008), may serve as a relatively reliable indicator for export productivity for site MD012404. As reported by Broecker and Clark (1999), planktonic foraminiferal derived $CaCO_3$ (larger than 63 μm) accounts for about 55% of total $CaCO_3$ in sites with water depth shallower than CCD. Thus the co-variations between FFA and $CaCO_3$ (Fig. 3e and f), although size differences among foraminiferal species may exist, further suggested that $CaCO_3$ record can also be used to infer productivity history from site MD012404.

The sedimentary $P_{react.}$ reflects bioavailable phosphorus in the euphotic zone that fueled export productivity (Anderson et al., 2001; Filippelli, 2008; Schoepfer et al., 2015). Phosphorus enters into the marine metabolic cycle through algal photosynthesis, during which dissolved inorganic phosphate is transformed into organic matter with the C:P ratio of ca. 106:1 (Redfield ratio). After formation, most of this organic matter is remineralized and recycled in the upper ocean; Only a few organic matter fractions, in the form of particulate organic matter, descend into the deep water and finally reaches the sea floor. During sedimentary burial, part of this organic P, which is labile, experiences digenesis and can be transformed into Fe bound/absorbed inorganic P and Ca bound apatite-P, and permanently sequestered in sediments (see supplementary materials) (Anderson et al., 2001; Faul et al., 2005; Filippelli, 2008; Kraal et al., 2017). The residual refractory organic P is ultimately buried into the sediment. Hence, the sum of organic P, Fe bound/absorbed inorganic P and Ca bound apatite-P was termed as reactive P and was used to indicate export productivity (Anderson et al., 2001; Li et al., 2017b). Reactive P (Fig. 3g) displays similar pattern with

FFA and $CaCO_3$ from core MD012404 over the last 30 kyr. As the preservation of $P_{react.}$ and $CaCO_3$ are sensitive to multiple, but different, environmental factors, hence the similar pattern of variations between these proxy records strongly supports their interpretation here as robust representation of changes in export productivity. As proposed by Li et al. (2017b), the evolution of North Pacific Intermediate Water exerted a major control on export productivity in the Okinawa Trough (for further details, see the supplementary materials).

Using simple binary endmember model and $\delta^{13}C_{TOC}$ data, OC_{marine} content was calculated for site MD012404. The OC_{Marine} record showed higher values during the last glacial maximum and deglacial stages but lower values in the last 9 kyr. The temperate variation of OC_{Marine} record is similar to that of TOC but is deviated from that of productivity records, e.g., reactive phosphorus and planktonic FFA, over the last 30 kyr. Sedimentary TOC flux had been used to reflect biological productivity in the Okinawa Trough (Dou et al., 2015; Kao et al., 2005). However, organic carbon burial have been questioned because it is sensitive to diagenesis that controlled by environment redox state.

Compared to Fe, Mn is a more redox-sensitive and mobilizing element. Under well-oxygenated environments, Mn (III) and Mn (IV) occur as insoluble oxyhydroxides. While in oxygen-depleted environments, reduced Mn (II), which is soluble and remobilizable, forms (Calvert and Pedersen, 1996). Thus, the presence of Mn-excess suggests an oxygenated state and Mn-depletion suggests a reducing environment condition. During the Holocene, higher Mn/Al ratios (Fig. 2e) suggest high oxidation state of water-sediment interface for site MD012404, which is not favoring for organic matter preservation. By contrast, negative shift of Mn/Al ratios occurred during the last deglacial and glacial stages (Fig. 2e), suggesting reduced condition that favoring for organic matter burial. Published sedimentary total sulfur records (Fig. 4b and c) from the middle Okinawa trough lends further support to the Okinawa trough redox change as indicated by Mn/Al record (Kao et al., 2006a; Lim et al., 2017). In the following section, we proposed a new proxy to decipher the temporal variation of organic carbon burial efficiency and controlling mechanisms in the middle Okinawa Trough over the last glacial-interglacial cycle, and we also provide a conceptual model to reconcile the inconsistency between biological pump and organic carbon burial.

5.2. Organic carbon burial and $OC_{marine}/P_{react.}$ as a proxy for burial efficiency

During the sedimentary burial process, portion of organic matter is decomposed and carbon is released in the form of dissolved inorganic carbon while inorganic phosphorus released from organic matter is absorbed or reincorporated in authigenic minerals as described above. Thus, by assuming that the marine sourced organic matter has a constant C:P ratio (mol/mol) prior to decomposition on the sea floor as supported by constant sinking particle $OC/P_{react.}$ ratio (mol/mol) through the water column (Faul et al., 2005), the downcore variability of $OC_{marine}/P_{react.}$ was used to reflect the organic carbon burial efficiency (OCBE) with higher values suggest better preservation and vice versa for more decomposition. As show in Fig. 4e, the $OC_{marine}/P_{react.}$ values from site MD012404 fall in the range of 28–81, obviously lower than averaged $OC/P_{react.}$ (C:P = 187) value of global ocean sinking particles (Faul et al., 2005), and/or Redfield ratio (C:P = 106), suggesting preferential removal of OC_{marine} relative to reactive phosphorus during burial processes. As for the general pattern, the $OC_{marine}/P_{react.}$ ratios paced the variation of Mn/Al and total sulfur records (Fig. 4b, c and d), with higher $OC_{marine}/P_{react.}$ values, i.e., good organic carbon preservation, occurred during the last glacial and deglacial stages and low values, i.e., poor organic carbon preservation, occurred through the mid-late Holocene.

Variation of OCBE was in parallel with carbonate ($CaCO_3$) preservation record, i.e., FFI, from the same core (Fig. 4f). As discussions in Section 5.1, core MD012404 lies above the modern carbonate compensation depth (Fig. 1e). Thus the poor preservation, break down in other words, of foraminiferal shells should be ascribed to processes occurred in the sediment. Previous studies show that sedimentary biogenic $CaCO_3$ dissolves in response to respiration, i.e., decomposition of organic matter, in the top few centimeters of sediment from site lies above the saturation horizon (Archer et al., 1989; Broecker, 2009). Thus, the co-variation of $OC_{marine}/P_{react.}$ and FFI records suggests that the organic carbon burial efficiency, as indicated by $OC_{marine}/P_{react.}$ ratio, was controlled by diagenesis occured in the sediment.

It has been reported that clay mineral protection and high sedimentation are favoring for organic carbon preservation (Blair and Aller, 2012; Katsev and Crowe, 2015; Lopes et al., 2015). However in core MD012404, the general pattern of $OC_{marine}/P_{react.}$, i.e., higher values in glacial-deglacial and low values in the middle-late Holocene, did not paces that of the sediment linear sedimentation rate (LSR), sediment mass accumulation rate (MAR) or clay mineral content over the last 30 kyr (see Supplementary Fig. S2). In addition, we did not find any significant X-Y correlations between $OC_{marine}/P_{react.}$ and sediment LSR, MAR, or clay mineral records (see supplementary Fig. S3). Thus, the oxygen exposure time during sedimentation and clay mineral protection were unlikely the dominant controlling factors for OCBE in the middle Okinawa Trough over the last 30 kyr.

Today, the vertical water circulation and euphotic productivity was closely related with the intrusion of Kuroshio Current into the Okinawa Trough. On the one hand, the intrusion of Kuroshio Current leads to stronger deep water ventilation resulting in higher bottom water O_2 concentration in the Okinawa Trough (Fig. 1b). On the other hand, the Kuroshio Current also induces intermediate water upwelling around the East China Sea continental slope/shelf providing nutrient for phytoplankton growth therein (Chen, 1996). However, the topography surrounding Okinawa Trough makes sea level change an important factor to modulate the flow path and intensity of the Kuroshio Current on different climate background. Evidence from planktonic foraminifer *P. obliquiloculata* abundance and sedimentary mercury as well as numerical model all suggested that the Kuroshio Current intrusion/intensity into the Okinawa Trough was significantly reduced during the LGM and early deglaciation when sea level in low state (Chang et al., 2008; Kao et al., 2005, 2006b; Lim et al., 2017; Xiang et al., 2007). According to our data and proxies re-examination above, we summarized a conceptual diagram for the Okinawa Trough (Fig. 4) emphasizing different oxygenation statuses induced by water exchange and organic carbon burial efficiency during three time intervals: Stage I (14.5–24.0 ka, LGM and Heinrich stadial 1), Stage II (8.0–14.5 ka, including Bølling-Allerød, Younger Dryas and early Holocene) and Stage III (0.5–8.0 ka, mid-late Holocene).

During the Stage I (14.5–24.0 ka), the North Pacific Deep Water shallower than 1500 m was more oxygenated (Fig. 4a) relative to the late Holocene (Galbraith and Jaccard, 2015), which was caused by weakening upper oceanic soft tissue pump and increased O_2 dissolution in cooler waters (Galbraith and Jaccard, 2015; Jaccard and Galbraith, 2012). Meanwhile, euphotic productivity was lower in the middle Okinawa Trough (Li et al., 2017b). However, the 100–130 m sea level drop (Fig. 4i) significantly reduced the intrusion and intensity of Kuroshio Current into the Okinawa Trough (Fig. 4g, h) as indicated by POA (Chang et al., 2008; Xiang et al., 2007;), geochemical proxies (Diekmann et al., 2008; Lim et al., 2017), and numerical models (Kao et al., 2006b; Zheng et al., 2016), leading to weakened vertical mixing and reduced deep water ventilation with Philippine Sea through Kerama Gap (Kao et al., 2005; Lim et al., 2017). In addition, short distance between the paleo-river estuaries and the Okinawa Trough increased freshwater discharge to our site as indicated by reduced sea surface water salinity (Chen et al., 2010); and this further favoring water stratification. Thus, the middle Okinawa Trough basin was characterized by less oxygenated bottom/pore water as indicated by Mn (Fig. 4d) and total sulfur (Fig. 4b and c), favoring sediment organic carbon preservation (Fig. 4e). From 14.5 to 8.0 ka, i.e., Stage II, the

North Pacific water shallower than 1500 m experienced large oxygenation variability (Fig. 4a), displaying low, high and low oxygen states during Bølling-Allerød, Younger Dryas and early Holocene respectively (Galbraith and Jaccard, 2015; Jaccard and Galbraith, 2012). However, the OCBE record did not response accordingly, and the $OC_{marine}/P_{react.}$ experienced gradual decreasing and is in parallel with gradual sea level rise (Fig. 4e and i). Sea level rose gradually from about −100 m at 14.5 ka to −12 m at 8.0 ka (Fig. 4i) during this interval, favoring gradual intrusion and strengthening of Kuroshio Current (Fig. 4g and h) into the Okinawa Trough and hence better bottom water ventilation (Kao et al., 2005; Lim et al., 2017); ultimately, this resulted in negative relationship between OCBE and global sea level in general (see supplementary Fig. S3d). Whereas export productivity experienced rapid increase from 13 to 9 ka (Fig. 3), contrasting to the decreasing trend of OCBE, hence it was excluded from major controlling factors for organic carbon burial in the middle Okinawa Trough. During the Stage III (0–8 kyr interval), the upper North Pacific Ocean water O_2 concentration (Fig. 4a) was higher than that during stage II (averaged) but still lower than that during Stage I (Galbraith and Jaccard, 2015; Jaccard and Galbraith, 2012 and reference therein). Whereas the Okinawa Trough was characterized by highest deep water oxygenation (Mn/Al ration, Fig. 4d). During this period, the sea level reaches the modern condition, and the main axis of the Kuroshio Current shifted back to the middle Okinawa Trough (Fig. 4g and h) (Diekmann et al., 2008; Kao et al., 2006b; Lim et al., 2017; Xiang et al., 2007), and freshwater input to the middle Okinawa Trough decreased (Chen et al., 2010). This enhanced vertical water mixing and better deep water ventilation (Kao et al., 2005; Lim et al., 2017) through the Kerama Gap resulting in higher bottom water O_2 concentration (Fig. 4c and d) and poor organic carbon preservation (Fig. 4e). Although primary productivity was highest during the Holocene in the middle Okinawa Trough (Fig. 3e and g), organic carbon burial (Fig. 3b and c) was lowest due to the highest bottom water oxygenation state. In summary, variations of sea level and related Kuroshio Current main axis shift determined the glacial-deglacial-Holocene pattern of bottom-water/surface-sediment redox condition in the middle Okinawa Trough over the last 24 kyr, and this ultimately controlled variation of organic carbon preservation therein.

5.3. Sea level modulated organic carbon preservation in China marginal seas

By adding new data, we extended our preservation record for site MD012404 spanning the entire 91 kyr (Fig. 5). POA varied in parallel with global sea level change and experienced low values during 14–24 ka and 60–70 ka (Fig. 5b and d), suggesting reduced/weakened Kuroshio Current intrusion/intensity into the Okinawa Trough. In accordance, preservation records, FFI and $OC_{marine}/P_{react.}$ (Fig. 5e and f), experienced similar changes through the past 91 kyr with better preservation occurred in 14–24 ka and 60–70 ka, but poor preservation during the Holocene. Taken together, we find that preservation records varied in sync with that of POA and sea level records on orbital time scales. This suggests that sea level change dominated the general variation of organic matter preservation in the middle Okinawa trough over the last 91 kyr.

Similar to the Okinawa Trough, the South China Sea (SCS) is a semi-closed basin with deep water exchange with Philippine Sea through Luzon Strait. Previous studies show that glacial sea-level drop significantly reduced SCS deep water ventilation (Li et al., 2017a; Löwemark et al., 2009; Wan and Jian, 2014). Using published data, we found similar variations of sedimentary preservation records from the middle Okinawa Trough and the northern SCS during the last glacial-interglacial cycle (Fig. 5f and g). For example, carbonate preservation in the middle Okinawa trough exhibit similar pattern with that from the northern SCS deep sea cores, which displaying as good preservation during glacial periods and poor preservation during interglacial periods (Chen et al., 1997). In addition, our $OC_{marine}/P_{react.}$ record also displays similar variation of $OC/P_{react.}$ from one northern SCS core (ODP site 1144; 20°3.18′N, 117°25.14′E; water depth 2037 m) although terrestrial contribution to TOC was not evaluated in the original research (Tamburini et al., 2003). Proxy records for evaluating terrestrial vs marine contributions, e.g., TOC-$\delta^{13}C$ and BIT, all suggest northern SCS deep-sea sediment TOC was dominated by marine sourced components (Kienast et al., 2001; Li et al., 2013), and glacial marine sourced contribution even increased (Kienast et al., 2001). Hence, variability of $OC/P_{react.}$ from the northern SCS was not controlled by variation of terrestrial input and the variability of $OC/P_{react.}$ could be used as that for $OC_{marine}/P_{react.}$. Taking together, it is reasonable to postulate that sea level modulated organic carbon preservation in both middle Okinawa Trough and the northern SCS. By compilation organic carbon data from hundreds of sediment cores, Cartapanis et al. (2016) provided that the global organic carbon burial paralleled with the global sea level change on glacial-interglacial cycles, displaying as glacial high values and interglacial low values (Fig. 5b and c). Despite the potential of nutrients supply mechanisms to explain the temporal pattern of organic carbon burial (Cartapanis et al., 2016; Kohfeld et al., 2005; Martínez-García et al., 2014), we suggest that global sea level change might also play an important role in controlling organic burial through modulating organic carbon preservation efficiency especially in marginal seas with semi-closed basins (Wang, 1999).

5.4. Implications

In the eastern North Pacific region to the west of Oregon, organic carbon burial rate and its burial efficiency were also found to be decoupled with euphotic export productivity (Lopes et al., 2015). However, differed from our case, sedimentation rate was the major controller on burial rate and efficiency for organic carbon in the Oregon case (Lopes et al., 2015). Although the controlling factors were different, the decoupling phenomenon suggests that organic carbon burial is not a simple function of primary or export productivity. This reminds us to be cautious in evaluating biological pump using geological organic carbon records or organic biomarkers. In addition, plenty of climate models have been applied to predict ocean's biological pump and its role in regulating atmosphere CO_2 (Schmittner et al., 2008). However, some models only considering water column transfer efficiency which was controlled by column temperature and sinking velocity (Marsay et al., 2015). Results from our case and the Oregon case suggest that the inclusion of geographically different environmental factors, such as deep circulation and sedimentation rate, is needed for model optimization and better prediction on longer time scales, i.e., hundreds to thousands of years.

6. Conclusions

In summary, we made analysis of metal elements and planktonic foraminifer assemblages from site MD012404 located in the middle Okinawa Trough. By combining with published productivity and environmental data from the same core, discussions on variations of export productivity, water column redox condition, and organic carbon burial in the middle Okinawa Trough were carried out. Main conclusions are summarized as follows:

(1) Reactive phosphorus and planktonic foraminiferal fauna assemblages were used as export productivity proxies in the middle Okinawa Trough over the last 30 kyr, which indicate that productivity was low during the last glacial stage but was high during the Holocene. Export productivity in the Okinawa Trough was modulated by the penetration depth of North Pacific Intermediate Water.

(2) We proposed a proxy, i.e., $OC_{marine}/P_{react.}$, for evaluating marine sourced organic carbon burial efficiency in the middle Okinawa Trough. Variability of $OC_{marine}/P_{react.}$ suggests organic carbon

burial efficiency was high during glacial and deglacial stages and low during the middle-late Holocene, and is decoupled with euphotic export productivity. Marine sourced organic carbon burial efficiency in the middle Okinawa Trough was controlled by sea level change through modulating the intrusion and intensity of the Kuroshio Current into the Okinawa Trough.

(3) The phenomenon that decoupled primary/export productivity with organic carbon burial was observed in both western and eastern North Pacific marginal regions since the last glacial stage, referring us to take caution when using sedimentary organic carbon or organic biomarkers to infer paleo-productivity history.

Acknowledgements

We thank Shih-Chieh Hsu for metal analysis in Research Center for Environmental Changes (Academia Sinica, Taipei, Taiwan). The manuscript was greatly improved by comments from two anonymous reviewers, and by editor Gert J. De Lange. This work was supported by National Natural Science Foundation of China (NSFC, Grant No. 41503069, 41721005, 91328207, and 41176059), and by the National Basic Research Program of China (973 Program, Grant No. 2015CB954003). The authors wish to dedicate this work to the memory of Da-Wei's father, Yankuan Li, a great farmer. This is MEL (State Key Laboratory of Marine Environmental Science) publication 2018255.

Appendix A. Supplementary materials

Supplementary data to this article can be found online at https://doi.org/10.1016/j.margeo.2018.02.013.

References

Amano, A., Itaki, T., 2016. Variations in sedimentary environments in the forearc and backarc regions of the Ryukyu Arc since 25 ka based on CNS analysis of sediment cores. Quat. Int. 397, 360–372.
Anderson, L.D., Delaney, M.L., Faul, K.L., 2001. Carbon to phosphorus ratios in sediments: implications for nutrient cycling. Glob. Biogeochem. Cycles 15, 65–79.
Archer, D., Emerson, S., Reimers, C., 1989. Dissolution of calcite in deep-sea sediments: pH and O_2 microelectrode results. Geochim. Cosmochim. Acta 53, 2831–2845.
Arndt, S., Jørgensen, B.B., LaRowe, D.E., Middelburg, J.J., Pancost, R.D., Regnier, P., 2013. Quantifying the degradation of organic matter in marine sediments: a review and synthesis. Earth Sci. Rev. 123, 53–86.
Bassinot, F.C., Baltzer, A., Chen, M.T., DeDeckker, P., Khuhnt, W., Levitan, M., Nurnberg, D., Oba, T., Prentice, M., Sarnthein, M., Situmorang, M., Tiedemann, R., Holbourn, A., Kiefer, T., Pflaumann, U., Rothe, S., 2002. Scientific Report of the WEPAMA Cruise, MD122/IMAGES VII. pp. 453.
Bereiter, B., Eggleston, S., Schmitt, J., Nehrbass-Ahles, C., Stocker, T.F., Fischer, H., Kipfstuhl, S., Chappellaz, J., 2015. Revision of the EPICA Dome C CO_2 record from 800 to 600 kyr before present. Geophys. Res. Lett. 42, 542–549.
Blair, N.E., Aller, R.C., 2012. The fate of terrestrial organic carbon in the marine environment. Annu. Rev. Mar. Sci. 4, 401–423.
Broecker, W.S., 2009. Wally's quest to understand the Ocean's $CaCO_3$ cycle. Annu. Rev. Mar. Sci. 1, 1–18.
Broecker, W.S., Clark, E., 1999. $CaCO_3$ size distribution: a paleocarbonate ion proxy? Paleoceanography 14, 596–604.
Brumsack, H.-J., 2006. The trace metal content of recent organic carbon-rich sediments: implications for cretaceous black shale formation. Palaeogeogr. Palaeoclimatol. Palaeoecol. 232, 344–361.
Burdige, D.J., 2007. Preservation of organic matter in marine sediments: controls, mechanisms, and an imbalance in sediment organic carbon budgets? Chem. Rev. 107, 467–485.
Calvert, S.E., Pedersen, T.F., 1996. Sedimentary geochemistry of manganese; implications for the environment of formation of manganiferous black shales. Econ. Geol. 91, 36–47.
Cartapanis, O., Bianchi, D., Jaccard, S.L., Galbraith, E.D., 2016. Global pulses of organic carbon burial in deep-sea sediments during glacial maxima. Nat. Commun. 7, 10796.
Chang, Y.-P., Wu, S.-M., Wei, K.-Y., 2005. Foraminiferal oxygen isotope stratigraphy and high-resolution organic carbon, carbonate records from the Okinawa Trough (IMAGES MD012404 and ODP Site 1202). Terr. Atmos. Ocean. Sci. 16, 57–73.
Chang, Y.-P., Wang, W.-L., Yokoyama, Y., Matsuzaki, H., Kawahata, H., Chen, M.-T., 2008. Millennial-scale Planktic foraminifer faunal variability in the East China Sea during the past 40000 years (IMAGES MD012404 from the Okinawa Trough). Terr. Atmos. Ocean. Sci. 19, 389–401.
Chang, Y.-P., Chen, M.-T., Yokoyama, Y., Matsuzaki, H., Thompson, W.G., Kao, S.-J., Kawahata, H., 2009. Monsoon hydrography and productivity changes in the East China Sea during the past 100,000 years: Okinawa Trough evidence (MD012404). Paleoceanography 24, PA3208.
Chen, C.-T.A., 1996. The Kuroshio intermediate water is the major source of nutrients on the East China Sea continental shelf. Oceanol. Acta 19, 523–527.
Chen, M.-T., Huang, C.-Y., Wei, K.-Y., 1997. 25,000-year late quaternary records of carbonate preservation in the South China Sea. Palaeogeogr. Palaeoclimatol. Palaeoecol. 129, 155–169.
Chen, M.T., Lin, X.P., Chang, Y.P., Chen, Y.C., Lo, L., Shen, C.C., Yokoyama, Y., Oppo, D.W., Thompson, W.G., Zhang, R., 2010. Dynamic millennial-scale climate changes in the northwestern Pacific over the past 40,000 years. Geophys. Res. Lett. 37, L23603.
Costa, K.M., Jacobel, A.W., McManus, J.F., Anderson, R.F., Winckler, G., Thiagarajan, N., 2017. Productivity patterns in the equatorial Pacific over the last 30,000 years. Glob. Biogeochem. Cycles 31, 850–865.
Dickson, A.G., 1990. Thermodynamics of the dissociation of boric acid in synthetic seawater from 273.15 to 318.15 K. Deep Sea Res. Part A 37, 755–766.
Dickson, A.G., Millero, F.J., 1987. A comparison of the equilibrium constants for the dissociation of carbonic acid in seawater media. Deep Sea Res. Part A 34, 1733–1743.
Diekmann, B., Hofmann, J., Henrich, R., Fütterer, D.K., Röhl, U., Wei, K.-Y., 2008. Detrital sediment supply in the southern Okinawa trough and its relation to sea-level and Kuroshio dynamics during the late quaternary. Mar. Geol. 255, 83–95.
Dou, Y., Yang, S., Li, C., Shi, X., Liu, J., Bi, L., 2015. Deepwater redox changes in the southern Okinawa Trough since the last glacial maximum. Prog. Oceanogr. 135, 77–90.
Faul, K.L., Paytan, A., Delaney, M.L., 2005. Phosphorus distribution in sinking oceanic particulate matter. Mar. Chem. 97, 307–333.
Filippelli, G.M., 2008. The global phosphorus cycle: past, present, and future. Elements 4, 89–95.
Galbraith, E.D., Jaccard, S.L., 2015. Deglacial weakening of the oceanic soft tissue pump: global constraints from sedimentary nitrogen isotopes and oxygenation proxies. Quat. Sci. Rev. 109, 38–48.
Gao, S., Luo, T.-C., Zhang, B.-R., Zhang, H.-F., Han, Y.-W., Zhao, Z.-D., Hu, Y.-K., 1998. Chemical composition of the continental crust as revealed by studies in East China. Geochim. Cosmochim. Acta 62, 1959–1975.
Glasby, G.P., Notsu, K., 2003. Submarine hydrothermal mineralization in the Okinawa Trough, SW of Japan: an overview. Ore Geol. Rev. 23, 299–339.
Grant, K.M., Rohling, E.J., Bar-Matthews, M., Ayalon, A., Medina-Elizalde, M., Ramsey, C.B., Satow, C., Roberts, A.P., 2012. Rapid coupling between ice volume and polar temperature over the past 150,000 years. Nature 491, 744–747.
Hedges, J.I., Keil, R.G., 1995. Sedimentary organic matter preservation: an assessment and speculative synthesis. Mar. Chem. 49, 81–115.
Hedges, J.I., Keil, R.G., Benner, R., 1997. What happens to terrestrial organic matter in the ocean? Org. Geochem. 27, 195–212.
Hsu, S.-C., Lin, F.-J., Jeng, W.-L., Chung, Y.-c., Shaw, L.-M., 2003. Hydrothermal signatures in the southern Okinawa Trough detected by the sequential extraction of settling particles. Mar. Chem. 84, 49–66.
Jaccard, S.L., Galbraith, E.D., 2012. Large climate-driven changes of oceanic oxygen concentrations during the last deglaciation. Nat. Geosci. 5, 151–156.
Jian, Z., Chen, R., Li, B., 1996. Deep-sea benthic foraminiferal record of the paleoceanography in the southern Okinawa Trough over the last 20,000 years. Sci. China Ser. D Earth Sci. 39, 551–560.
Jian, Z., Wang, P., Saito, Y., Wang, J., Pflaumann, U., Oba, T., Cheng, X., 2000. Holocene variability of the Kuroshio Current in the Okinawa Trough, northwestern Pacific Ocean. Earth Planet. Sci. Lett. 184, 305–319.
Kao, S.J., Horng, C.S., Hsu, S.C., Wei, K.Y., Chen, J., Lin, Y.S., 2005. Enhanced deepwater circulation and shift of sedimentary organic matter oxidation pathway in the Okinawa Trough since the Holocene. Geophys. Res. Lett. 32, L15609.
Kao, S.J., Roberts, A.P., Hsu, S.C., Chang, Y.P., Lyons, W.B., Chen, M.T., 2006a. Monsoon forcing, hydrodynamics of the Kuroshio Current, and tectonic effects on sedimentary carbon and sulfur cycling in the Okinawa Trough since 90 ka. Geophys. Res. Lett. 33, L05610.
Kao, S.J., Wu, C.-R., Hsin, Y.-C., Dai, M., 2006b. Effects of sea level change on the upstream Kuroshio Current through the Okinawa Trough. Geophys. Res. Lett. 33, L16604.
Katsev, S., Crowe, S.A., 2015. Organic carbon burial efficiencies in sediments: the power law of mineralization revisited. Geology 43, 607–610.
Key, R.M., Kozyr, A., Sabine, C.L., Lee, K., Wanninkhof, R., Bullister, J.L., Feely, R.A., Millero, F.J., Mordy, C., Peng, T.H., 2004. A global ocean carbon climatology: results from Global Data Analysis Project (GLODAP). Glob. Biogeochem. Cycles 18, GB4031.
Kienast, M., Calvert, S.E., Pelejero, C., Grimalt, J.O., 2001. A critical review of marine sedimentary $\delta^{13}C_{org}$-pCO_2 estimates: new Palaeorecords from the South China Sea and a revisit of other low-latitude $\delta^{13}C_{org}$-pCO_2 records. Glob. Biogeochem. Cycles 15, 113–127.
Kohfeld, K.E., Chase, Z., 2011. Controls on deglacial changes in biogenic fluxes in the North Pacific Ocean. Quat. Sci. Rev. 30, 3350–3363.
Kohfeld, K.E., Quéré, C.L., Harrison, S.P., Anderson, R.F., 2005. Role of marine biology in glacial-interglacial CO_2 cycles. Science 308, 74–78.
Kraal, P., Dijkstra, N., Behrends, T., Slomp, C.P., 2017. Phosphorus burial in sediments of the sulfidic deep Black Sea: key roles for adsorption by calcium carbonate and apatite authigenesis. Geochim. Cosmochim. Acta 204, 140–158.
Lambeck, K., Rouby, H., Purcell, A., Sun, Y., Sambridge, M., 2014. Sea level and global ice volumes from the Last Glacial Maximum to the Holocene. Proc. Natl. Acad. Sci. 111, 15296–15303.
Li, T., Xiang, R., Sun, R., Cao, Q., 2005. Benthic foraminifera and bottom water evolution in the middle-southern Okinawa Trough during the last 18 ka. Sci. China Ser. D Earth Sci. 48, 805–814.
Li, D., Zhao, M., Tian, J., Li, L., 2013. Comparison and implication of TEX_{86} and $U^{K'}_{37}$ temperature records over the last 356 kyr of ODP site 1147 from the northern South

China Sea. Palaeogeogr. Palaeoclimatol. Palaeoecol. 376, 213–223.
Li, D., Chiang, T.-L., Kao, S.-J., Hsin, Y.-C., Zheng, L.-W., Yang, J.-Y.T., Hsu, S.-C., Wu, C.-R., Dai, M., 2017a. Circulation and oxygenation of the glacial South China Sea. J. Asian Earth Sci. 138, 387–398.
Li, D., Zheng, L.-W., Jaccard, S.L., Fang, T.-H., Paytan, A., Zheng, X., Chang, Y.-P., Kao, S.-J., 2017b. Millennial-scale ocean dynamics controlled export productivity in the subtropical North Pacific. Geology 45, 651–654.
Liang, W.D., Tang, T.Y., Yang, Y.J., Ko, M.T., Chuang, W.S., 2003. Upper-ocean currents around Taiwan. Deep-Sea Res. II Top. Stud. Oceanogr. 50, 1085–1105.
Lim, D., Kim, J., Xu, Z., Jeong, K., Jung, H., 2017. New evidence for Kuroshio inflow and deepwater circulation in the Okinawa Trough, East China Sea: sedimentary mercury variations over the last 20 kyr. Paleoceanography 32, 571–579.
Lin, Y.-S., Wei, K.-Y., Lin, I.-T., Yu, P.-S., Chiang, H.-W., Chen, C.-Y., Shen, C.-C., Mii, H.-S., Chen, Y.-G., 2006. The Holocene *Pulleniatina* minimum event revisited: geochemical and faunal evidence from the Okinawa Trough and upper reaches of the Kuroshio current. Mar. Micropaleontol. 59, 153–170.
Lopes, C., Kucera, M., Mix, A.C., 2015. Climate change decouples oceanic primary and export productivity and organic carbon burial. Proc. Natl. Acad. Sci. 112, 332–335.
Löwemark, L., Steinke, S., Wang, C.-H., Chen, M.-T., Müller, A., Shiau, L.-J., Kao, S.-J., Song, S.-R., Lin, H.-L., Wei, K.-Y., 2009. New evidence for a glacioeustatic influence on deep water circulation, bottom water ventilation and primary productivity in the South China Sea. Dyn. Atmos. Oceans 47, 138–153.
Marsay, C.M., Sanders, R.J., Henson, S.A., Pabortsava, K., Achterberg, E.P., Lampitt, R.S., 2015. Attenuation of sinking particulate organic carbon flux through the mesopelagic ocean. Proc. Natl. Acad. Sci. 112, 1089–1094.
Martínez-García, A., Sigman, D.M., Ren, H., Anderson, R.F., Straub, M., Hodell, D.A., Jaccard, S.L., Eglinton, T.I., Haug, G.H., 2014. Iron fertilization of the Subantarctic Ocean during the last Ice Age. Science 343, 1347–1350.
McLennan, S.M., 2001. Relationships between the trace element composition of sedimentary rocks and upper continental crust. Geochem. Geophys. Geosyst. 2, 1021.
Nakamura, H., Nishina, A., Liu, Z., Tanaka, F., Wimbush, M., Park, J.-H., 2013. Intermediate and deep water formation in the Okinawa Trough. J. Geophys. Res. C: Oceans 118, 6881–6893.
Nelson, D.M., Tréguer, P., Brzezinski, M.A., Leynaert, A., Quéguiner, B., 1995. Production and dissolution of biogenic silica in the ocean: revised global estimates, comparison with regional data and relationship to biogenic sedimentation. Glob. Biogeochem. Cycles 9, 359–372.
Pelletier, G., Lewis, E., Wallace, D., 2005. A Calculator for the CO_2 System in Seawater for Microsoft Excel/VBA. Washington State Department of Ecology, Olympia, WA, Brookhaven National Laboratory, Upton, NY, USA.
Roth, R., Ritz, S.P., Joos, F., 2014. Burial-nutrient feedbacks amplify the sensitivity of atmospheric carbon dioxide to changes in organic matter remineralisation. Earth Syst. Dyn. 5, 321–343.
Ruan, J., Xu, Y., Ding, S., Wang, Y., Zhang, X., 2017. A biomarker record of temperature and phytoplankton community structure in the Okinawa Trough since the last glacial maximum. Quat. Res. 1–9.
Schlitzer, R., 2016. Ocean Data View. Available on. https://odv.awi.de/.
Schmittner, A., Oschlies, A., Matthews, H.D., Galbraith, E.D., 2008. Future changes in climate, ocean circulation, ecosystems, and biogeochemical cycling simulated for a business-as-usual CO_2 emission scenario until year 4000 AD. Glob. Biogeochem. Cycles 22, GB1013.
Schoepfer, S.D., Shen, J., Wei, H., Tyson, R.V., Ingall, E., Algeo, T.J., 2015. Total organic carbon, organic phosphorus, and biogenic barium fluxes as proxies for paleomarine productivity. Earth Sci. Rev. 149, 23–52.
Shao, H., Yang, S., Wang, Q., Guo, Y., 2015. Discriminating hydrothermal and terrigenous clays in the Okinawa Trough, East China Sea: evidences from mineralogy and geochemistry. Chem. Geol. 398, 85–96.
Shao, H., Yang, S., Cai, F., Li, C., Liang, J., Li, Q., Hyun, S., Kao, S.-J., Dou, Y., Hu, B., Dong, G., Wang, F., 2016. Sources and burial of organic carbon in the middle Okinawa Trough during late Quaternary paleoenvironmental change. Deep-Sea Res. I Oceanogr. Res. Pap. 118, 46–56.
Sigman, D.M., Boyle, E.A., 2000. Glacial/interglacial variations in atmospheric carbon dioxide. Nature 407, 859–869.
Spindler, M., Hemleben, C., Salomons, J.B., Smit, L.P., 1984. Feeding behavior of some planktonic foraminifers in laboratory cultures. J. Foraminifer. Res. 14, 237–249.
Tamaki, K., Honza, E., 1991. Global tectonics and formation of marginal basins: role of the western Pacific. Episodes 14, 224–230.
Tamburini, F., Adatte, T., Föllmi, K., Bernasconi, S.M., Steinmann, P., 2003. Investigating the history of East Asian monsoon and climate during the last glacial–interglacial period (0–140,000 years): mineralogy and geochemistry of ODP Sites 1143 and 1144, South China Sea. Mar. Geol. 201, 147–168.
Tsuji, T., Takai, K., Oiwane, H., Nakamura, Y., Masaki, Y., Kumagai, H., Kinoshita, M., Yamamoto, F., Okano, T., Kuramoto, S., 2012. Hydrothermal fluid flow system around the Iheya North Knoll in the mid-Okinawa trough based on seismic reflection data. J. Volcanol. Geotherm. Res. 213-214, 41–50.
Ujiié, H., Hatakeyama, Y., Gu, X.X., Yamamoto, S., Ishiwatari, R., Maeda, L., 2001. Upward decrease of organic C/N ratios in the Okinawa Trough cores: proxy for tracing the post-glacial retreat of the continental shore line. Palaeogeogr. Palaeoclimatol. Palaeoecol. 165, 129–140.
Ujiié, Y., Asahi, H., Sagawa, T., Bassinot, F., 2016. Evolution of the North Pacific subtropical gyre during the past 190 kyr through the interaction of the Kuroshio Current with the surface and intermediate waters. Paleoceanography 31, 1498–1513.
Wan, S., Jian, Z., 2014. Deep water exchanges between the South China Sea and the Pacific since the last glacial period. Paleoceanography 29, 2013PA002578.
Wang, P., 1999. Response of western Pacific marginal seas to glacial cycles: paleoceanographic and sedimentological features. Mar. Geol. 156, 5–39.
Winckler, G., Anderson, R.F., Jaccard, S.L., Marcantonio, F., 2016. Ocean dynamics, not dust, have controlled equatorial Pacific productivity over the past 500,000 years. Proc. Natl. Acad. Sci. 113, 6119–6124.
World Ocean Atlas, 2009. Available on. http://www.nodc.noaa.gov/OC5/WOA09/woa09data.html.
Wu, Y., Zhang, J., Liu, S.M., Zhang, Z.F., Yao, Q.Z., Hong, G.H., Cooper, L., 2007. Sources and distribution of carbon within the Yangtze River system. Estuar. Coast. Shelf Sci. 71, 13–25.
Xiang, R., Sun, Y., Li, T., Oppo, D.W., Chen, M., Zheng, F., 2007. Paleoenvironmental change in the middle Okinawa trough since the last deglaciation: evidence from the sedimentation rate and planktonic foraminiferal record. Palaeogeogr. Palaeoclimatol. Palaeoecol. 243, 378–393.
Xu, Z., Li, T., Nan, Q., Yu, X., Li, A., Choi, J., 2012. Paleoenvironmental changes in the northern Okinawa trough since 25 ka BP: REE and organic carbon evidence. J. Earth Sci. 23, 297–310.
Yang, S., Jung, H.-S., Li, C., 2004. Two unique weathering regimes in the Changjiang and Huanghe drainage basins: geochemical evidence from river sediments. Sediment. Geol. 164, 19–34.
Yu, J., Elderfield, H., 2007. Benthic foraminiferal B/Ca ratios reflect deep water carbonate saturation state. Earth Planet. Sci. Lett. 258, 73–86.
Zhai, S., Yu, Z., Du, T., 2007. Elemental geochemical records of seafloor hydrothermal activities in the sediments from the Okinawa Trough. Acta Oceanol. Sin. 26, 53–62.
Zheng, X., Li, A., Kao, S., Gong, X., Frank, M., Kuhn, G., Cai, W., Yan, H., Wan, S., Zhang, H., Jiang, F., Hathorne, E., Chen, Z., Hu, B., 2016. Synchronicity of Kuroshio Current and climate system variability since the Last Glacial Maximum. Earth Planet. Sci. Lett. 452, 247–257.